ELSEVIER

Journal of Photochemistry and Photobiology A: Chemistry 128 (1999) 129–133

Journal of Photochemistry and Photobiology A:Chemistry

www.elsevier.nl/locate/jphotochem

Synthesis and photocatalytic properties of $HNbWO_6/TiO_2$ and $HNbWO_6/Fe_2O_3$ nanocomposites

Jihuai Wu [a], Satoshi Uchida [b], Yoshinobu Fujishiro [b], Shu Yin [b], Tsugio Sato [b,*]

[a] *Institute of Material Physical Chemistry, Huaqiao University, Quanzhou 362011, China*
[b] *Institute for Chemical Reaction Science, Tohoku University, Sendai 980-8577, Japan*

Received 25 January 1999; received in revised form 7 July 1999; accepted 14 July 1999

Abstract

TiO_2 and Fe_2O_3 were intercalated into the interlayer of $HNbWO_6$ together with Pt by the successive reactions of $HNbWO_6$ with $[Pt(NH_3)_4]Cl_2$, *n*-$C_3H_7NH_2$ and acidic TiO_2 colloid solution or $[Fe_3(CH_3CO_2)_7(OH)(H_2O)_2]NO_3$ aqueous solution followed by UV light irradiation. The height of TiO_2 and Fe_2O_3 pillars was less than 0.5 nm. The bandgap energies of $HNbWO_6/TiO_2$ and $HNbWO_6/Fe_2O_3$ nanocomposites were 3.12 and 2.22 eV, respectively. Both nanocomposites showed hydrogen production activity by the bandgap irradiation in the presence of sacrificial hole acceptor such as methanol. The photocatalytic activities of $HNbWO_6/TiO_2$ and $HNbWO_6/Fe_2O_3$ nanocomposites were superior to those of unsupported TiO_2 and Fe_2O_3 and were enhanced by co-incorporation of Pt. The hydrogen production activities of $HNbWO_6$/Pt, $HNbWO_6$/(Pt, TiO_2), $HNbWO_6/Fe_2O_3$ and $HNbWO_6$/(Pt, Fe_2O_3) under UV light irradiation were much lower than that of unsupported TiO_2/Pt, however, they showed photocatalytic activity even under visible light irradiation.

Keywords: Photocatalyst; Visible light; $HNbWO_6$; TiO_2; Fe_2O_3; Intercalation; Nanocomposites

1. Introduction

Photocatalytic reactions of semiconductors, such as splitting of water and reduction of carbon dioxide, have received special attention because of their possible application for the conversion of solar energy into chemical energy. Many studies have been carried out to enhance the photocatalytic activity of semiconductors. It is to be expected that the photoactivity of a semiconductor increases with the decrease of particle size since, in such a system, the distance which the photoinduced holes and electrons have to diffuse before reaching the interface decreases. Consequently, the holes and electrons can be effectively captured by the electrolyte in the solution [1]. Incorporation of semiconductor particles via chemical reactions in the interlayer region of a lameller compound is a promising method for the fabrication of a nanocomposite consisting of host layers with ultrafine particles in the interlayer. Yamanaka et al. [2], Enea and Bard [3], Yoneyama et al. [4–6], and Sato et al. [7–9] have reported the incorporation of extremely small particles of Fe_2O_3, TiO_2, CdS and CdS–ZnS mixtures, <1 nm in thickness, into the interlayer of layered compounds, such as montmorillonite, layered double hydroxides, layered niobate and layered titanate. As expected, the photocatalytic activities of the incorporated semiconductors were much higher than those of unsupported semiconductors. In previous papers [7,8], we reported that the photoactivities of incorporated semiconductors depended on the physico-chemical properties of the host layer. In continuation of our studies, new layered nanocomposites, $HNbWO_6/TiO_2$ and $HNbWO_6/Fe_2O_3$ were synthesized and their photocatalytic activities were evaluated.

2. Experimental section

2.1. Chemicals

$HNbWO_6$ was prepared by the proton exchange reaction of $LiNbWO_6$ in 2 M HNO_3 at room temperature for 48 h with one intermediate replacement of the acid in 24 h. $LiNbWO_6$ was obtained by calcining stoichiometric mixture of Li_2CO_3, WO_3 and Nb_2O_5 at 800°C in air for 24 h with one intermediate grinding [10]. $[Fe_3(CH_3COO)_7(OH)(H_2O)_2]NO_3$ was

* Corresponsing author. Tel: +81-22-217-5597; fax: +81-22-217-5599
E-mail address: tsusato@icrs.tohoku.ac.jp (T. Sato)

1010-6030/99/$ – see front matter
PII: S1010-6030(99)00157-4

synthesized by the reaction of $Fe(NO_3)_3{\cdot}9H_2O$ with acetic anhydride in ethanol as reported [2]. Unsupported TiO_2 (Deggusa P-25) was commercially obtained and used without further purification. Unsupported TiO_2/Pt was obtained by the photodeposition of 0.3 wt.% Pt on P-25 by dispersing the powder in $Pt(NH_3)_4Cl_2$ solution, followed by UV light irradiation from a 100 W high pressure mercury lamp for 16 h. Unsupported Fe_2O_3 was prepared by adding a 1 M $Fe(NO_3)_3$ aqueous solution (50 ml) to a 5 M NH_3 aqueous solution (500 ml) at room temperature and the precipitate was washed with water until free of NH_3 and dried at 120°C.

2.2. Incorporation of TiO_2 and Pt into the interlayer of $HNbWO_6$

TiO_2 sol was made by adding titanium tetraisopropoxide to 1 M HCl solution with the TiO_2/HCl molar ratio of 0.25. $HNbWO_6$/*n*-$C_3H_7NH_2$ was obtained by stirring $HNbWO_6$ (1 g) in 50 ml of 20 vol% *n*-$C_3H_7NH_2$/*n*-heptane solution under reflux at 50°C for 72 h. $HNbWO_6$/*n*-$C_3H_7NH_2$ was added to TiO_2 sol solution with the TiO_2/$HNbWO_6$ molar ratio of 20. The suspension was continuously stirred for 6 h at room temperature so as to incorporate TiO_2 into the interlayer of $HNbWO_6$. After being filtered and washed with water, the specimen was dispersed in water and irradiated with UV light from a 450 W high-pressure mercury lamp at 60°C for 12 h so as to decompose any *n*-$C_3H_7NH_2$ remaining in the interlayer of $HNbWO_6$. The sample obtained was designated as $HNbWO_6/TiO_2$.

$[Pt(NH_3)_4]^{2+}$ was incorporated in the interlayer of $HNbWO_6$ by stirring $HNbWO_6$ (4 g) in 0.6 mM $[Pt(NH_3)_4]Cl_2$ aqueous solution (1000 ml) at room temperature for 72 h. After being filtered and washed with water, the specimen was dispersed in water and irradiated with UV light from a 450 W high-pressure mercury lamp at room temperature for 5 h to deposit Pt particles in the interlayer of $HNbWO_6$. The product obtained was designated as $HNbWO_6$/Pt. After that TiO_2 was incorporated into the interlayer of $HNbWO_6$/Pt by successive intercalating reactions with 20 vol% *n*-$C_3H_7NH_2$/*n*-heptane solution, TiO_2 sol solution and irradiation with UV light in a similar manner as that for preparing $HNbWO_6/TiO_2$. The sample obtained was designated as $HNbWO_6$/(Pt, TiO_2).

2.3. Incorporation of Fe_2O_3 and Pt into the interlayer of $HNbWO_6$

Fe_2O_3 was incorporated into the interlayer of $HNbWO_6$ by irradiating the $[Fe_3(CH_3CO_2)_7(OH)(H_2O)_2]^+$ exchanged compound with UV light from a 450 W high-pressure mercury lamp at 50°C for 12 h. The exchanged compound was obtained by ion-exchange reaction with $HNbWO_6$/*n*-$C_3H_7NH_2$ (2 g) and $[Fe_3(CH_3CO_2)_7(OH)(H_2O)_2]NO_3$ (25 g) in 500 ml water at 50°C for 72 h. The sample obtained was designated as $HNbWO_6/Fe_2O_3$.

Fe_2O_3 was incorporated into $HNbWO_6$/Pt by successive intercalating reactions with 20 vol% *n*-$C_3H_7NH_2$/*n*-heptane solution, $[Fe_3(CH_3CO_2)_7(OH)(H_2O)_2]NO_3$ aqueous solution and photodecomposition of $[Fe_3(CH_3CO_2)_7(OH)(H_2O)_2]^+$ in a similar manner as that for preparing $HNbWO_6/Fe_2O_3$. The sample obtained was designated as $HNbWO_6$/(Pt, Fe_2O_3).

2.4. Analysis

The crystalline phases of the products were identified by X-ray diffraction (Shimadzu XD-01) using graphite monochromized Cu Kα radiation. The chemical compositions of the products were determined by TG-DTA analysis (Rigaku Denki TAS 200 TG-DTA) and by inductively coupled plasma atomic emission spectroscopy (Seiko SPS-1200A) by dissolving the samples in water after mixing 0.1 g samples with 4 g Na_2CO_3 and calcining at 800°C for 4 h. The band gap energies of the products were determined from the onset of diffuse reflectance spectra of the powders measured by using a Shimadzu Model UV-2000 UV–VIS spectrophotometer. The specific surface areas of samples were determined by nitrogen gas adsorption method (Quantachrome Autosorb-1).

2.5. Photocatalytic reaction

Photocatalytic reaction was carried out in a Pyrex reactor of 1250 ml capacity attached to an inner radiation type 450 W high-pressure mercury lamp. The inner cell had thermostat water flowing through a jacket between the mercury lamp and the reaction chamber. The inner cell was constructed of Pyrex glass which served to filter out the UV emission of the mercury arc below 290 nm. The UV emission of the mercury arc below 400 nm was filtered out by flowing 1 M $NaNO_2$ solution between the mercury lamp and the reaction chamber. The photoactivity of the catalyst was determined by measuring the volume of hydrogen gas evolved with a gas burette when the suspension of catalyst was irradiated.

3. Results and discussions

3.1. Intercalation of TiO_2 or Fe_2O_3 into the interlayer of $HNbWO_6$

Fig. 1 depicts the X-ray powder diffraction patterns of the products (a) $HNbWO_6$, (b) $HNbWO_6$/*n*-$C_3H_7NH_2$, (c) $HNbWO_6$/Pt, (d) $HNbWO_6/Fe_2O_3$, (e) $HNbWO_6$/(Pt, Fe_2O_3), (f) $HNbWO_6/TiO_2$, (g) $HNbWO_6$/(Pt, TiO_2). The peak positions, corresponding to (110) of $HNbWO_6$, of samples (b)–(g) changed significantly depending on the species in the interlayer. These results suggested that the layered structure of $HNbWO_6$ was retained after intercalation of

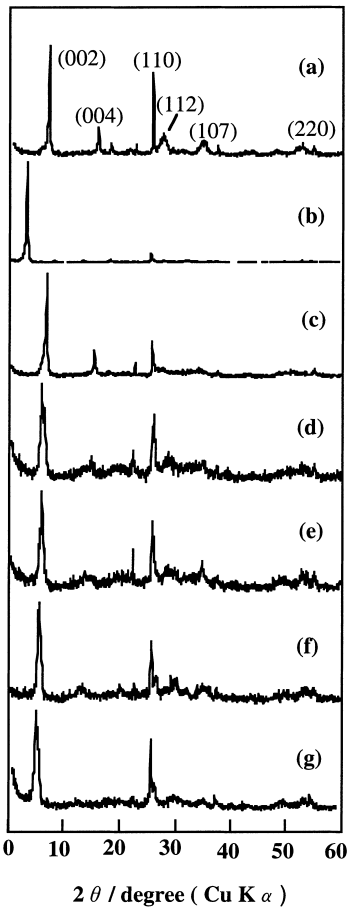

Fig. 1. Powder X-ray diffraction patterns of (a) $HNbWO_6$, (b) $HNbWO_6$/*n*-$C_3H_7NH_2$, (c) $HNbWO_6$/Pt, (d) $HNbWO_6$/Fe_2O_3, (e) $HNbWO_6$/(Pt, Fe_2O_3), (f) $HNbWO_6$/TiO_2, (g) $HNbWO_6$/(Pt, TiO_2).

n-$C_3H_7NH_2$, TiO_2, Fe_2O_3 and Pt, although the distance of the interlayer changed. Compared with sample (a), the main peak, corresponding to (002) of $HNbWO_6$ of sample (b), shifted significantly to lower 2θ angle, which indicated the expansion of the interlayer by incorporation of *n*-$C_3H_7NH_2$. The gallery height of $HNbWO_6$/*n*-$C_3H_7NH_2$ determined by subtracting the $HNbWO_6$ layer thickness (0.76 nm) [10,11], is 1.03 nm, which is almost twice the length of the *n*-$C_3H_7NH_2$ molecule. Therefore, it is suspected that two molecules of *n*-$C_3H_7NH_2$ are vertically arranged in the interlayer of $HNbWO_6$.

The TG curve of $C_3H_7NH_3NbWO_6$ (Fig. 2) indicated 14% weight loss until 650°C, which agreed with the calculated value (14%) according to the following reaction.

$$C_3H_7NH_3NbWO_6 + \tfrac{9}{2}O_2 \rightarrow \tfrac{1}{2}Nb_2O_5 + WO_3 + 3CO_2 + NH_3 + \tfrac{7}{2}H_2O$$

Therefore, it was confirmed that the stoichiometric amount of *n*-$C_3H_7NH_2$ was intercalated in $HNbWO_6$.

The reflection spectra of $HNbWO_6$, $HNbWO_6$/Pt, $HNbWO_6$/Fe_2O_3, $HNbWO_6$/(Pt, Fe_2O_3), $HNbWO_6$/TiO_2 and $HNbWO_6$/(Pt, TiO_2) are shown in Fig. 3. The spectra of

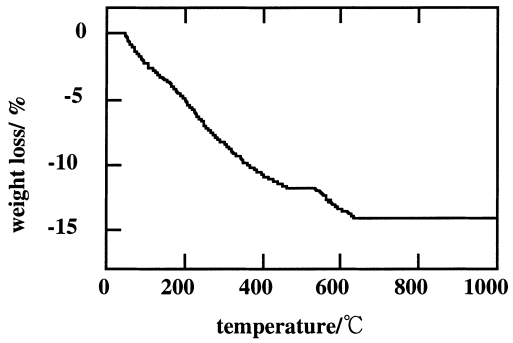

Fig. 2. TG curve of $HNbWO_6$/*n*-$C_3H_7NH_2$.

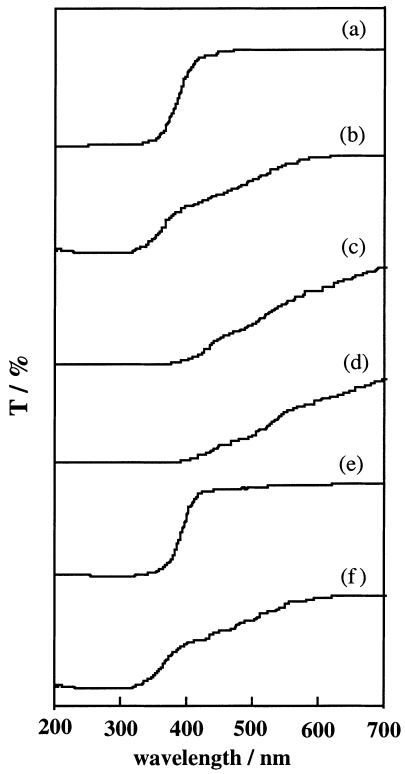

Fig. 3. Reflection spectra of (a) $HNbWO_6$, (b) $HNbWO_6$/Pt, (c) $HNbWO_6$/Fe_2O_3, (d) $HNbWO_6$/(Pt, Fe_2O_3), (e) $HNbWO_6$/TiO_2, (f) $HNbWO_6$/(Pt, TiO_2).

$HNbWO_6$ and $HNbWO_6$/TiO_2 were almost the same, indicating the onset at ca. 400 nm (3.10 eV). On the other hand, $HNbWO_6$/Fe_2O_3 and $HNbWO_6$/(Pt, Fe_2O_3) showed broad reflection spectra with two onsets at ca. 400 and 550 nm corresponding to both the host $HNbWO_6$ layer and incorporated Fe_2O_3. The different phenomena that occurred on incorporation of Fe_2O_3 and TiO_2 might be due to the difference in band gap energies, i.e., the difference in the band gap energies of TiO_2 and $HNbWO_6$ is not large, but that of Fe_2O_3 and $HNbWO_6$ is large. Similar phenomena were also observed in $H_2Ti_4O_9$-TiO_2, $H_4Nb_6O_{17}$-TiO_2, $H_2Ti_4O_9$-Fe_2O_3 and $H_4Nb_6O_{17}$-Fe_2O_3 systems [8]. It is also notable that although $HNbWO_6$ and $HNbWO_6$/TiO_2 were white, both

Table 1
Gallery heights, element contents, band gap energies and surface areas of the products

Product	Gallery height (nm)	Content (wt.%)			Band gap energy (eV)	Surface area ($m^2\ g^{-1}$)
		Ti	Fe	Pt		
$HNbWO_6$	0.29	0	0	0	3.10	5.99
$HNbWO_6$/Pt	0.31	0	0	0.13	3.10, 2.25	7.08
$HNbWO_6/TiO_2$	0.49	4.42	0	0	3.10	36.1
$HNbWO_6/Fe_2O_3$	0.43	0	4.01	0	3.10, 2.25	23.3
$HNbWO_6$/(Pt, TiO_2)	0.51	3.55	0	0.28	3.10, 2.25	36.1
$HNbWO_6$/(Pt, Fe_2O_3)	0.43	0	2.55	0.13	3.10, 2.25	23.3

$HNbWO_6$/Pt and $HNbWO_6$/(Pt, TiO_2) showed yellow coloring and two onsets at ca. 400 and 550 nm. It was reported that $HTaWO_6$ which possesses the same crystal structure as $HNbWO_6$ caused photo-induced phase transformation to Ta_2O_5 and WO_3 on laser irradiation [12]. Therefore, it was suspected that similar photo-induced phase transformation occurred in $HNbWO_6$/Pt and $HNbWO_6$/(Pt, TiO_2) systems to form Nb_2O_5 and WO_3, since both samples were irradiated with UV light for 5 and 12 h for the photodeposition of Pt and photodecomposition of n-$C_3H_7NH_2$ in the interlayer, respectively (see Section 2.2). So that, the onset at 400 and 550 nm might be attributed to the $HNbWO_6$ remaining and WO_3 formed by the photo-induced phase transformation. Since no noticeable transformation was observed in $HNbWO_6/TiO_2$ which was irradiated with UV light for 12 h, it is suspected that Pt promoted the photo-induced phase transformation of $HNbWO_6$.

The gallery heights, amounts of Ti, Fe and Pt elements incorporated, band gap energies and the specific surface areas of products are summarized in Table 1. The amounts of Ti, Fe and Pt elements incorporated were 3.55–4.42, 2.55–4.01 and 0.13–0.28 wt.%, respectively. Since the gallery heights of $HNbWO_6/TiO_2$ and $HNbWO_6/Fe_2O_3$ were 0.49 nm and 0.43 nm, the thickness of TiO_2 and Fe_2O_3 in the interlayer of $HNbWO_6$ was suggested to be less than 0.5 nm. The specific surface areas of $HNbWO_6/TiO_2$, $HNbWO_6/Fe_2O_3$, $HNbWO_6$/(Pt, TiO_2) and $HNbWO_6$/(Pt, Fe_2O_3) were 4–6 times greater than that of $HNbWO_6$ which further indicated the formation of the Fe_2O_3 and TiO_2 pillars.

3.2. Photocatalytic properties

The amount of hydrogen gas produced from 1250 ml of 10 vol% methanol solutions containing 1 g of dispersed unsupported TiO_2 (P-25), unsupported TiO_2/Pt, $HNbWO_6$, $HNbWO_6$/Pt, $HNbWO_6/TiO_2$, $HNbWO_6$/(Pt, TiO_2), unsupported Fe_2O_3, $HNbWO_6/Fe_2O_3$, and $HNbWO_6$/(Pt, Fe_2O_3) at 60°C when irradiated with the light ($\lambda > 290$ nm) from a 450 W mercury arc for 5 h are shown in Fig. 4(a). All samples showed photocatalytic activity to evolve hydrogen gas. The amount of hydrogen gas produced increased in the sequence, unsupported Fe_2O_3 < unsupported TiO_2 (P-25) < $HNbWO_6$ < $HNbWO_6/Fe_2O_3$ < $HNbWO_6/TiO_2$ < $HNbWO_6$/(Pt, Fe_2O_3) < $HNbWO_6$/(Pt, TiO_2) ≪ TiO_2/Pt. These results suggested that the photocatalytic activities of Fe_2O_3 and TiO_2 were enhanced when they were intercalated in the interlayer of $HNbWO_6$, especially when Pt is intercalated together with them. Under the experimental conditions, the amounts of hydrogen gas

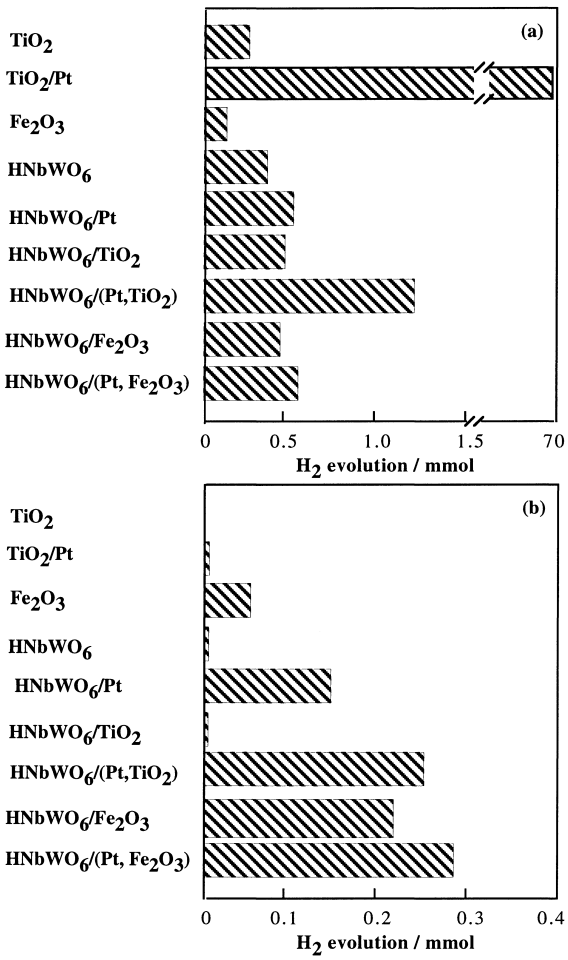

Fig. 4. Amount of hydrogen gas produced from 1250 ml of 10 vol% methanol solution containing 1 g of dispersed unsupported TiO_2 (P-25), $HNbWO_6$, $HNbWO_6$/Pt, $HNbWO_6/TiO_2$, $HNbWO_6$/(Pt, TiO_2), unsupported Fe_2O_3, $HNbWO_6/Fe_2O_3$, and $HNbWO_6$/(Pt, Fe_2O_3) at 60°C by irradiating a 450 W mercury arc above (a) 290 nm and (b) 400 nm for 5 h.

produced from $HNbWO_6/TiO_2$ and $HNbWO_6$/(Pt, TiO_2) catalyst were about 2 and 5.5 times larger than that of unsupported TiO_2. The amounts of hydrogen gas produced from $HNbWO_6$/(Pt, TiO_2) catalyst, however, was only 2% of Pt deposited P-25. This perhaps can be attributed to low content of TiO_2 in $HNbWO_6$/(Pt, TiO_2) (3.5 wt.% see Table 1) and greater difficulty of the hole scavenger, CH_3OH, accessing the intercalated semiconductor.

Fig. 4(b) expresses the amount of hydrogen gas from 1250 ml of 10 vol% methanol solution containing 1 g of dispersed samples at 60°C under visible light irradiation($\lambda > 400$ nm) from a 450 W mercury arc for 5 h. As expected from their wide band gap energies (>3 eV), no hydrogen gas evolution was observed in the presence of unsupported TiO_2, unsupported TiO_2/Pt, $HNbWO_6$ and $HNbWO_6/TiO_2$. It was notable that evolution of hydrogen gas in the presence of $HNbWO_6/Fe_2O_3$ was three times greater than that of unsupported Fe_2O_3 and was greatly enhanced by co-intercalation of Pt with Fe_2O_3. The enhancement of hydrogen evolution by incorporation in the interlayer indicates that photoinduced electrons and holes in intercalated Fe_2O_3 can be effectively used for the reduction of water and oxidation of methanol, but those in unsupported Fe_2O_3 rapidly recombined. The depression of the recombination of electrons and holes might be due to the electron transfer from Fe_2O_3 to host layer and/or Pt. Similar results were reported in Fe_2O_3-Pt-$H_4Nb_6O_{17}$ and Fe_2O_3-Pt-$H_2Ti_4O_9$ systems, but the photocatalytic activity of $HNbWO_6$/(Pt, Fe_2O_3) catalyst was ca. 1.5 and 1.7 times greater than that of $H_4Nb_6O_{17}$/(Pt, Fe_2O_3) and $H_2Ti_4O_9$/(Pt, Fe_2O_3), respectively [7]. It was also notable that both $HNbWO_6$/Pt and $HNbWO_6$/(Pt, TiO_2) showed photocatalytic activity under visible light irradiation. Since both $HNbWO_6$ and TiO_2 are wide band gap semiconductors, it is suspected that WO_3 formed in those samples by photo-induced phase transformation played important roles in the hydrogen evolution under visible light irradiation. The photocatalytic activity under visible light irradiation was in the order $HNbWO_6$/(Pt, Fe_2O_3) > $HNbWO_6$/(Pt, TiO_2) > $HNbWO_6/Fe_2O_3$ > $HNbWO_6$/Pt ≫ unsupported Fe_2O_3.

4. Conclusions

From the results of tests described, the following conclusions may be drawn. (1) TiO_2 and Fe_2O_3 together with Pt could be intercalated into the interlayer of $HNbWO_6$ by successive reactions of $HNbWO_6$ with $[Pt(NH_3)_4]Cl_2$, *n*-$C_3H_7NH_2$, acidic TiO_2 colloid solution or $[Fe_3(CH_3CO_2)_7(OH)(H_2O)_2]NO_3$ aqueous solution followed by UV light irradiation. (2) The thickness of TiO_2 and Fe_2O_3 was less than 0.5 nm. (3) The hydrogen production activity of $HNbWO_6/TiO_2$ and $HNbWO_6/Fe_2O_3$ nanocomposites was superior to that of unsupported TiO_2 (P-25) and Fe_2O_3, respectively. (4) The photocatalytic activities of $HNbWO_6/TiO_2$ and $HNbWO_6/Fe_2O_3$ nanocomposites are greatly enhanced by co-intercalation of Pt.

Acknowledgements

This work was partly supported by a Grant-in-Aid for Scientific Research from the Ministry of Education, Science and Culture.

References

[1] A. Hagfeldt, M. Gratzel, Chem. Rev. 95 (1995) 49.
[2] S. Yamanaka, T. Doi, S. Sako, Mater. Res. Bull. 19 (1994) 61.
[3] O. Enena, A.J. Bard, J. Phys. Chem. 90 (1986) 301.
[4] H. Miyoshi, H. Yoneyama, J. Chem. Soc. Faraday Trans. 85 (1989) 1873.
[5] H. Yoneyama, S. Haga, S. Yamanaka, J. Phys. Chem. 93 (1989) 4833.
[6] H. Miyoshi, H. Mori, H. Yoneyama, Langmuir. 7 (1991) 503.
[7] T. Sato, Y. Yamamoto, S. Uchida, J. Chem. Soc. Faraday Trans. 92 (1996) 5089.
[8] S. Uchida, Y. Yamamoto, T. Sato, J. Chem. Soc. Faraday Trans. 93 (1997) 3229.
[9] T. Sato, K. Masaki, K. Sato, J. Chem. Tech. Biotechnol. 67 (1996) 339.
[10] V. Bhat, J. Gopalakrishnan, Solid State Ionics 26 (1988) 25.
[11] R.P. Shannon, C.T. Prewitt, Acta Cryst. B25 (1961) 125.
[12] E. Cazzanelli, G. Mariotto, M. Catti, Solid State Ionics 53 (1992) 383.